DYNAMIC MODELING OF ORGANIC RANKINE CYCLE (ORC) SYSTEM FOR FAULT DIAGNOSIS AND CONTROL SYSTEM DESIGN

Sungjin Choi[1] and Susan Krumdieck[1]

[1]University of Canterbury, Private Bag 4800, Christchurch 8140 New Zealand

sungjin.choi@pg.canterbury.ac.nz

susan.krumdieck@canterbury.ac.nz

Keywords: *Organic Rankine Cycle, Dynamic Modeling and Control, Moving Boundary Lumped Parameter Method*

ABSTRACT

Dynamic simulation plays an important role of providing a higher-level of process analysis of the system and supporting system configuration, operation, maintenance, diagnosis and design of the control system. The purpose of this research is to develop a virtual simulation tool for current suite of geothermal power plants. This article provides a numerical modeling framework for the dynamic modeling including detailed component models and a generic dynamic feedback control and fault diagnosis model for an organic Rankine cycle (ORC) system. A moving boundary method with switched system model is used to model time-varying performance of a heat exchanger in various flow conditions. A custom library for models of ORC components and system dynamic models has been built in Matlab/Simulink environment. The developed model is capable of designing a component- and system level control strategy and fault diagnosis system.

1. BACKGROUND

Renewable energy sources are making a major contribution to reduce global carbon emission and will make a great contribution to future global energy supplies and sustainable energy system. Growing price instability and insecurity of non-renewable energy such as fossil fuels due to its limited reserve stock and restricted geographical distribution leads investment invigoration and technological growth in renewable energy industry. Geothermal energy is a clean and sustainable renewable resource which has a vast amount of heat energy generated and stored in the earth. The temperature range of the geothermal fluid ranges from 50 to 350 ℃ but it is mostly below 150 ℃. Organic Rankine Cycles (ORCs) are capable of extracting and converting low enthalpy heat sources into electrical power by means of an organic working fluid, such as ammonia, pentane, hexane, R22 etc.

Design of an ORC system requires a robust understanding of its thermal and hydraulic components, system operating conditions and dynamic behaviors. Some of the key issues that need to be considered at the design stage are control system synthesis for process regulation and optimization, as well as start-up and shut down strategies. To achieve an integrated approach to the system design, all issues related to steady state and dynamic response of plant operation must be taken into account. Having a comprehensive understanding of the system is required not only for early development objectives but also for the purpose of maintaining optimum operating conditions.

A traditional steady state analysis is an essential tool for analysis of system operability and controllability and can be useful for capturing the slow dynamics of the system (hours, days, or years). However it is unable to describe short term transient behaviors in a cycle caused by varying operating conditions and unfavorable dynamics. A system might occasionally need to be operated in an unusual circumstance such as shut-down/ start-up or it sometimes experiences a decrease in performance due to the internal or external disturbance such as change of resource condition and system/component malfunction at the operating system level. As a plant undergoes such a transition, it is required to adjust and improve system performance and reconfigure the system and operation strategies. Dynamic simulation is capable of supporting analysis of the impact of the uncertainty on the system performance and detailed phase of design of the system and operation strategies. At the operation level, it would be an essential tool for fine-tuning of the plant and establishing a plan in the event of unusual operation such as shut-down/ start-up and system breakdown.

Unlike a static analysis and experimental study, limited research on dynamic modeling and control of an ORC system are available, especially in geothermal applications. Quoilin (Quoilin, Aumann, Grill, Schuster, Lemort & Spliethoff, 2011) presented dynamic model of a small scale ORC using volumetric expander and studied a control strategy against a varying heat source. Zhang (Zhang, Zhang, Hou & Fang, 2012) studied control strategies for the superheated temperature of an ORC process using generalized predictive control. Casella (Casella, Mathijssen, Colonna & Buijtenen, 2013) developed a software library of modular reusable dynamic models of ORC components under Modelica environment. Proctor (Proctor, Yu, Young, 2015) modeled an ORC system in geothermal application using the process simulator VMGSim and studied a control strategy for the position of valves located at the geothermal wellhead.

In this work, a moving boundary lumped parameter approach is adopted to model the dynamic aspects of the heat exchanger. A Matlab/Simulink based custom library has been developed as a dynamic simulation tool seeking to establish a model-based control-oriented modeling framework for ORC system. The final aim of the work is to explore underlying dynamics of ORC system in geothermal application focusing on operation and control strategies. The fault detection and isolation and fault tolerant control method on the system will also be addressed.

This paper outlines the modeling and simulation strategies of ORC system focusing on control and fault diagnosis system design purpose. The paper will examine in detail the heat exchanger model approach and the design of the

modeling tools. Simple example problem will be presented as a numerical test.

2. MODELING

A numerical framework in Matlab/Simulink platform for the generic dynamic feedback control model has been developed. The model uses a moving boundary lumped parameter approach to analyze the dynamics of heat exchanger. The modeling has been developed in state space form by linearizing around operating points to facilitate a control system design. Figure 1 shows a schematic diagram of the generic dynamic feedback control model. The model inputs are steady state design or operation data and empirical parameters of the components. The control strategy can be best analyzed and designed through considering a steady state aspects of the system along with an optimization model. The fault diagnosis and tolerant control scheme can then be applied into the control-oriented model. The model would provide any information necessary to system re-/configuration, control and operation strategy and fault diagnosis results. The design or reality-based plant model would be effectively implemented under the current modeling framework and is expected to be used for various purposes.

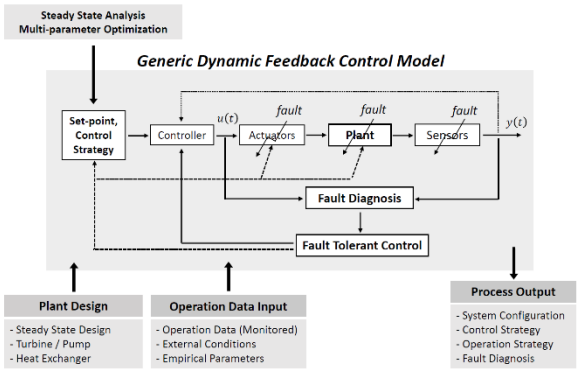

Figure 1. Generic dynamic feedback control model

	Definition		Definition
$\boldsymbol{\rho}$	density	$\boldsymbol{A_{i,o}}$	inner/outer surface
$\boldsymbol{p}$	pressure	$\boldsymbol{L}$	length
$\boldsymbol{h}$	enthalpy	$\boldsymbol{P}$	perimeter
$\boldsymbol{T}$	temperature	$\boldsymbol{V}$	volume
$\boldsymbol{\dot{m}}$	mass flow rate	$\boldsymbol{W}$	power
$\boldsymbol{\alpha}$	heat transfer coeff.	$\boldsymbol{\eta}$	efficiency
$\boldsymbol{\gamma}$	void fraction	**_a**	ambient
$\boldsymbol{x}$	vapor fraction	**_w**	wall
$\boldsymbol{C_p}$	specific heat	**_in**	inlet
$\boldsymbol{A}$	cross-sectional area	**_out**	outlet

Table 1 Nomenclature

In this section, a modeling method and design of the modeling tool are presented. A general case of the moving boundary approach for two-phase heat exchanger is illustrated with vapor and liquid conditions at inlet and outlet respectively. The model offers various modes of the heat exchanger based on the fluid condition around the heat exchanger. Table 1 shows a list of symbols and meanings used in this paper.

2.1 Organic Rankine Cycle

A fundamental principle of ORCs is same as Rankine cycle except the working fluid is an organic fluid instead of water. Figure 2 shows a schematic diagram of the standard ORC system. The thermodynamic processes are described on temperature-entropy diagram which is shown in Figure 3. The liquid state of working fluid undergoes an increase in pressure by the pump. In evaporator, the temperature of working fluid is increased in a liquid form until it reaches a slightly superheated state. The vapor state of working fluid expands through the turbine, generating electricity in the generator. Finally the vapor from the turbine turns it back into liquid state while traveling through the condenser.

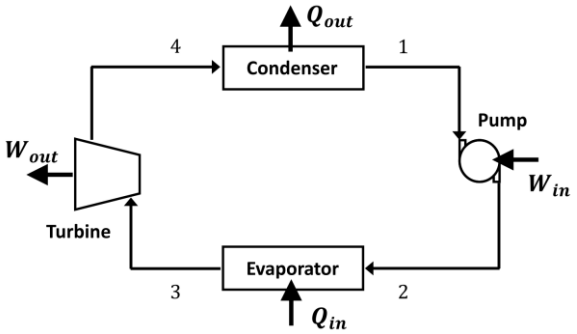

Figure 2. Basic configuration of Organic Rankine Cycle

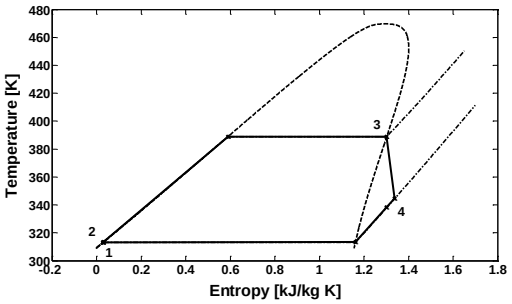

Figure 3 T-s diagram of Organic Rankine Cycle

2.2 Component Models

The dynamics of ORC system are assumed to be dominated by the dynamics of the heat exchanger. The dynamics of other components (e.g. expander, pump, valve, etc.) are generally an order of magnitude faster than the heat exchangers and are modeled with static relationship. Therefore the modeling of the heat exchanger is most critical part in modeling the ORC system. The heat exchanger components; evaporator, condenser, preheater and recuperator, can be modelled using moving boundary approaches (MacArthur & Grald, 1989, 1992). The moving boundary approach was rigorously studied by Alleyne's group for applications in a dynamic modeling of vapor compression cycle. (Eldredge, Rasmussen & Alleyne, 2008, Li & Alleyne, 2010, etc.). The moving boundary heat exchanger model captures dynamics of boundary between regions of different fluid state. The model is designed to facilitate low order control design models by simplifying two-phase flow problems into the type of lumped-parameter systems.

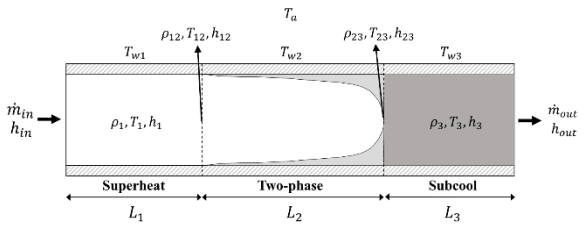

Figure 4. Schematic of moving boundary model (vapor condition at inlet, liquid condition at outlet)

Figure 4 shows schematic of three region (Superheated, Two-phase, Subcooled) moving boundary model of a condenser. The modeling approach can be applied to develop various modes of the heat exchanger such as evaporator, 2-region and single phase heat exchanger, etc. The transport of mass, momentum and energy for a fluid in the heat exchangers can be described by the conservation of the quantities being transported. It is assumed one dimensional fluid flow along a long circular tube and the pressure and viscous dissipation is negligible. Therefore the governing conservation laws for mass, energy of working fluid are respectively given by

$$\frac{\partial(\rho A)}{\partial t} + \frac{\partial(\dot{m})}{z} = 0 \qquad (\mathbf{1})$$

$$\frac{\partial(\rho A h - A p)}{\partial t} + \frac{\partial(\dot{m} h)}{\partial z} = P_i \alpha_i (T_w - T) \qquad (\mathbf{2})$$

where the subscript w indicates the heat exchanger wall. The energy equation for the wall is:

$$\left(C_p \rho V\right)_w \frac{\partial T_w}{\partial t} = \alpha_i A_i (T - T_w) + \alpha_o A_o (T_a - T_w) \qquad (\mathbf{3})$$

The conservation equations for each region are obtained by integrating over the superheated (from 0 to L_1), two-phase (from L_1 to $L_1 + L_2$) and subcooled region. (from $L_1 + L_2$ to L_T) using Leibniz's rule which is given by

$$\int_{z_1(t)}^{z_2(t)} \frac{\partial f(z,t)}{\partial t} dt = \frac{d}{dt}\int_{z_1(t)}^{z_2(t)} f(z,t) dz - f(z_2(t),t)\frac{d\left(z_2(t)\right)}{dt} + f(z_1(t),t)\frac{d\left(z_1(t)\right)}{dt} \qquad (\mathbf{4})$$

Therefore the mass and energy equations over the superheated region are given by

$$A\left(\rho_1 - \rho_g\right)\dot{L}_1 + AL_1\left[\left.\frac{\partial \rho_1}{\partial p}\right|_{h_1} + \frac{1}{2}\left.\frac{\partial \rho_1}{\partial p}\right|_{h_1}\frac{dh_g}{dp}\right]\dot{p} + \frac{1}{2}\left(\left.\frac{\partial \rho_1}{\partial p}\right|_{h_1}\right) AL_1\,\dot{h}_{in} = \dot{m}_{in} - \dot{m}_{12} \qquad (\mathbf{5})$$

$$A\left(\rho_1 h_1 - \rho_g h_g\right)\dot{L}_1 + AL_1\left[\left(\left.\frac{\partial \rho_1}{\partial p}\right|_{h_1} + \frac{1}{2}\left.\frac{\partial \rho_1}{\partial p}\right|_{h_1}\frac{dh_g}{dp}\right)h_1 + \frac{1}{2}\frac{dh_g}{dp}\rho_1 - 1\right]\dot{p} \quad + \frac{1}{2}AL_1\left[\rho_1 + \left(\left.\frac{\partial \rho_1}{\partial h_1}\right|_p\right)h_1\right]\dot{h}_{in} = \dot{m}_{in}h_{in} - \dot{m}_{12}h_g + \alpha_{i1}A_i\left(\frac{L_1}{L_T}\right)(T_{w1} - T_1) \qquad (\mathbf{6})$$

where $\rho_{12} = \rho_g,\ h_{12} = h_g$. The average properties in the superheated region are assumed

$$h_1 = \frac{h_{in} + h_g}{2}, \quad T_1 = f_T(p, h_1) \qquad (\mathbf{7})$$

The fluid properties in the two-phase region are estimated and modeled using the mean void fraction assumption.

$$\rho_2 = \rho_f(1 - \bar{\gamma}) + \rho_g(\bar{\gamma}),\ \ h_2 = h_f(1 - \bar{\gamma}) + h_g(\bar{\gamma}) \qquad (\mathbf{8})$$

Experimental correlations of void fraction have been studied and can be founded in a number of references. In this study, we assume slip ratio correlation and the Zivi's correlation (1964) is used to estimate slip ratio S.

$$\gamma = \frac{x}{x + (1-x)\left(\rho_g/\rho_f\right)S}, \qquad S = \left(\rho_f/\rho_g\right)^{1/3} \qquad (\mathbf{9})$$

The mean void fraction can then be calculated by integrating over the inlet and outlet quality of the two-phase region

$$\bar{\gamma} = \int_{x_{in}}^{x_{out}} \gamma(x) dx = \int_{x_{in}}^{x_{out}} \frac{x}{x + (1-x)\left(\rho_g/\rho_f\right)S} dx \qquad (\mathbf{10})$$

The mass and the energy balance for the two-phase are:

$$AL_2\left[\frac{d\rho_f}{dp}(1 - \bar{\gamma}) + \frac{d\rho_g}{dp}(\bar{\gamma})\right]\dot{p} + A\left(\rho_g - \rho_f\right)\dot{L}_1 + A\left(\rho_g - \rho_f\right)(\bar{\gamma})\,\dot{L}_2 = \dot{m}_{12} - \dot{m}_{23} \qquad (\mathbf{11})$$

$$A\left(\rho_g h_g - \rho_f h_f\right)\dot{L}_1 + AL_2\left[\frac{d(\rho_f h_f)}{dp}(1 - \bar{\gamma}) + \frac{d(\rho_g h_g)}{dp}(\bar{\gamma}) - 1\right]\dot{p} + A\,\bar{\gamma}\left(\rho_g h_g - \rho_f h_f\right)\dot{L}_2 = \dot{m}_{12}h_g - \dot{m}_{23}h_f + \alpha_{i2}A_i\left(\frac{L_2}{L_T}\right)(T_{w2} - T_2) \qquad (\mathbf{12})$$

where $\rho_{23} = \rho_f,\ h_{23} = h_f$. For the subcooled region, the average properties are assumed

$$h_3 = \frac{h_{out} + h_f}{2}, \qquad T_3 = f_T(p, h_3) \qquad (\mathbf{13})$$

Integration of the mass and energy equations over the subcooled region gives

$$AL_3\left[\left.\frac{\partial \rho_3}{\partial p}\right|_{h_3} + \frac{1}{2}\left.\frac{\partial \rho_3}{\partial h_3}\right|_p\frac{dh_f}{dp}\right]\dot{p} + \frac{1}{2}\left(\left.\frac{\partial \rho_3}{\partial h_3}\right|_p\right)AL_3\,\dot{h}_{out} + A\left(\rho_f - \rho_3\right)\left(\dot{L}_1 + \dot{L}_2\right) = \dot{m}_{23} - \dot{m}_{out} \qquad (\mathbf{14})$$

$$A\left(\rho_g h_g - \rho_3 h_3\right)\dot{L}_1 + A\left(\rho_f h_f - \rho_3 h_3\right)\dot{L}_2 + \frac{1}{2}AL_3\left[\rho_3 + \left(\left.\frac{\partial \rho_3}{\partial h_3}\right|_p\right)h_3\right]\dot{h}_{out} + AL_3\left[\left(\left.\frac{\partial \rho_3}{\partial p}\right|_{h_3} + \frac{1}{2}\left.\frac{\partial \rho_3}{\partial h_3}\right|_p\frac{dh_f}{dp}\right)h_3 + \frac{1}{2}\frac{dh_f}{dp}\rho_3 - 1\right]\dot{p} = \dot{m}_{23}h_f - \dot{m}_{out}h_{out} + \alpha_{i3}A_i\left(\frac{L_3}{L_T}\right)(T_{w3} - T_3) \qquad (\mathbf{15})$$

The energy equation for the heat exchanger wall describes that the rate of heat transfer between the wall and both the working fluid and secondary fluid must equal the rate of wall energy change due to temperature change. The wall equation for the each region is:

$$\left(C_p \rho V\right)_w \dot{T}_{w1} + \left(C_p \rho V\right)_w \left(\frac{T_{w1} - T_{w2}}{L_1}\right)\dot{L}_1 = \alpha_{i1}A_i(T_1 - T_{w1}) + \alpha_o A_o(T_a - T_{w1}) \qquad (\mathbf{16})$$

$$\left(C_p \rho V\right)_w \dot{T}_{w2} = \alpha_{i2}A_i(T_2 - T_{w2}) + \alpha_o A_o(T_a - T_{w2}) \qquad (\mathbf{17})$$

$$\left(C_p\rho V\right)_w \dot{T}_{w3} + \left(C_p\rho V\right)_w \left(\frac{T_{w2}-T_{w3}}{L_1}\right)\left(\dot{L}_1+\dot{L}_2\right) = \alpha_{i3}A_i(T_3-T_{w3}) + \alpha_o A_o(T_a-T_{w3}) \quad (18)$$

The system of equations can be rearranged into 7 equations with 7 state variables by eliminating dependent variables and written in the matrix form

$$\boldsymbol{Q}(x,u)\,\dot{\boldsymbol{x}} = \boldsymbol{R}(x,u)$$

$$\begin{cases}\dot{\boldsymbol{x}} = \boldsymbol{Q}^{-1}\boldsymbol{R} = \boldsymbol{F}(x,u)\\ \boldsymbol{y} = \boldsymbol{G}(x,u)\end{cases} \quad (19)$$

where

$$\boldsymbol{Q} = \begin{bmatrix} Q_{11} & 0 & Q_{13} & 0 & 0 & 0 & 0\\ Q_{21} & Q_{22} & Q_{23} & Q_{24} & 0 & 0 & 0\\ Q_{31} & Q_{32} & Q_{33} & Q_{34} & 0 & 0 & 0\\ Q_{41} & Q_{42} & Q_{43} & Q_{44} & 0 & 0 & 0\\ Q_{51} & 0 & 0 & 0 & Q_{55} & 0 & 0\\ 0 & 0 & 0 & 0 & 0 & Q_{66} & 0\\ Q_{71} & Q_{72} & 0 & 0 & 0 & 0 & Q_{77} \end{bmatrix} \qquad \boldsymbol{x} = \begin{bmatrix} L_1\\ L_2\\ p\\ h_{out}\\ T_{w1}\\ T_{w2}\\ T_{w3}\end{bmatrix}$$

$$\boldsymbol{R} = \begin{bmatrix} \dot{m}_{in}\left(h_{in}-h_g\right) + \alpha_{i1}A_i\left(\frac{L_1}{L_T}\right)(T_{w1}-T_1)\\ \dot{m}_{in}h_g - \dot{m}_{out}\,h_f + \alpha_{i2}A_i\left(\frac{L_2}{L_T}\right)(T_{w2}-T_2)\\ \dot{m}_{out}\left(h_f-h_{out}\right) + \alpha_{i3}A_i\left(\frac{L_3}{L_T}\right)(T_{w3}-T_3)\\ \dot{m}_{in}-\dot{m}_{out}\\ \alpha_{i1}A_i(T_1-T_{w1}) + \alpha_o A_o(T_a-T_{w1})\\ \alpha_{i2}A_i(T_2-T_{w2}) + \alpha_o A_o(T_a-T_{w2})\\ \alpha_{i3}A_i(T_3-T_{w3}) + \alpha_o A_o(T_a-T_{w3}) \end{bmatrix}$$

The elements of the matrix $\boldsymbol{Q}$ can be found in Appendix. The ODE system can simply be simulated by direct numerical integration. The model also can be linearized around the operating points x_o, u_o. The operating points (initial conditions for simulation) can be obtained by considering steady state solutions of the system. Then the 7^{th} order linear system can be written using state space representation as follows:

$$\begin{cases}\dot{\boldsymbol{x}} = \boldsymbol{A}\boldsymbol{x} + \boldsymbol{B}\boldsymbol{u}\\ \boldsymbol{y} = \boldsymbol{C}\boldsymbol{x} + \boldsymbol{D}\boldsymbol{u}\end{cases} \quad (20)$$

where

$$\boldsymbol{A} = \left[\boldsymbol{Q}|_{x_o,u_o}\right]^{-1}\left[\frac{\partial \boldsymbol{R}}{\partial \boldsymbol{x}}\Big|_{x_o,u_o}\right] \qquad \boldsymbol{B} = \left[\boldsymbol{Q}|_{x_o,u_o}\right]^{-1}\left[\frac{\partial \boldsymbol{R}}{\partial \boldsymbol{u}}\Big|_{x_o,u_o}\right]$$

$$\boldsymbol{C} = \frac{\partial \boldsymbol{G}}{\partial \boldsymbol{x}}\Big|_{x_o,u_o} \qquad \boldsymbol{D} = \frac{\partial \boldsymbol{G}}{\partial \boldsymbol{u}}\Big|_{x_o,u_o}$$

The input and output variables can be defined as

$$\boldsymbol{u} = \left[\dot{m}_{in}\ \ \dot{m}_{out}\ \ h_{in}\ \ T_{a,in}\ \ \dot{m}_a\right]^T$$

$$\boldsymbol{y} = \left[L_1\ \ L_2\ \ p\ \ h_{out}\ T_{w1}\ \ T_{w2}\ \ T_{w3}\ T_{a,out}\ \ T_{out}\ m\right]^T$$

The moving boundary model requires modification in the structure of the zones based on the operating conditions of the heat exchanger in the system. Figure 5 shows some of the model variations that can be derived using the same approach. Each model has a different mathematical formulation to be implemented.

The primary purpose of the dynamic model is to support operation planning and control strategy design, especially when the system needs to be operated in an unusual circumstance such as shut-down/ start-up or there are abrupt changes in the system conditions due to the internal or external disturbances. In such a case the heat exchanger may suffer a loss of superheated and/or subcooled region during the operation and the model would suddenly become unusable because the structure of the region in the model, representing the fluid conditions, does not change with time.

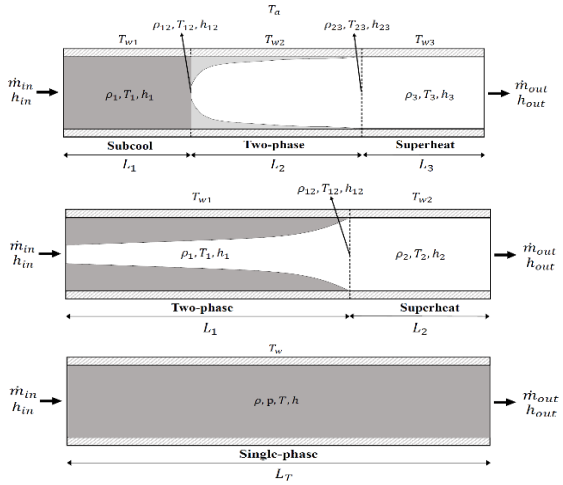

Figure 5 Model variations

McKinley (McKinley & Alleyne, 2008) suggested a switched model approach for heat exchangers to cope with the limitation of the original model. The current modelling tool has adopted the switched model to facilitate simulation of extreme operating conditions.

The response time of other components such as the turbine and pump is much faster than that of heat exchanger in the normal operating condition. Thus, a steady state model of the turbine and pump are generally used in a system model. The turbine model estimates the state of the outflow along with the generated mechanical power at given isentropic efficiency. The pressure is decreased along the component keeping mass flow rate constant. The first law of thermodynamics for the turbine is given by

$$W_{34} = \eta_G \dot{m}(h_3 - h_4) \quad (21)$$

$$\eta_{T,s} = \frac{h_3 - h_4}{h_3 - h_{4s}} \quad (22)$$

where h is an enthalpy, W_{34} is work done by the turbine. The generator efficiency is denoted by η_G. The subscript s refers to the isentropic process. The liquid pump model estimates the state of the outflow along with the required mechanical power consumption.

$$W_{12} = \dot{m}(h_1 - h_2) \quad (23)$$

The work input to the pump is denoted by W_{12}. The isentropic pump efficiency is defined as

$$\eta_{p,s} = \frac{h_1 - h_{2s}}{h_1 - h_2} \quad (24)$$

2.3 Fault Tolerant Control

An automated system control ensures the stability of the system and yields a pre-defined performance in the case where all system components operate safely. As the system increases in complexity, the risk of a fault in the system such as malfunctions in actuators, sensors or other system components increases, potentially resulting in performance degradation and instability of the system. Figure 6 shows the general type of the faults in the system.

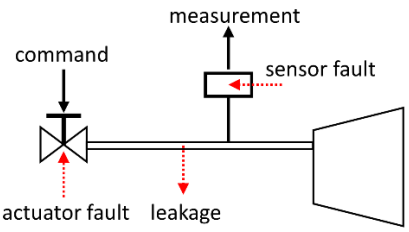

Figure 6 Type of faults

Fault-tolerant control (FTC) helps the system perform in normal operating conditions when taking into account the occurrence of faults. Most of the research work in FTC has been driven by the industry which involves mostly safety critical systems. With more emphasis from large-scale power plants on reliability, maintainability and survivability, attention to the FTC problem in industrial processes is also growing, but only a few related studies have been presented. Zhang (Zhang, Yue, 2006) provided a general review on the fault diagnosis and FTC method for power plants. The model based fault detection and tolerant control system has been developing which is applicable to dynamic model of ORC system.

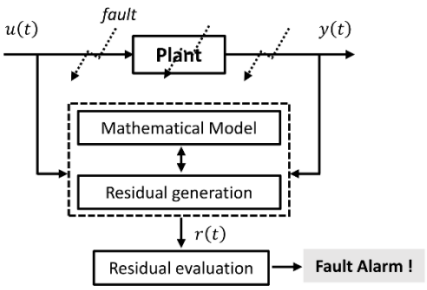

Figure 7 Model-based Fault Diagnosis Method

Figure 7 shows the structure of model-based fault diagnosis scheme which is the preceding stage of FTC scheme. The diagnosis process consists of three phases: Residual generation, evaluation and decision making. (Noura, Theilliol, Ponsart, Chamseddine, 2009). The diagnosis process provides information of magnitude and location of the fault over these phases. The FTC scheme then uses the information to compensate for the fault effect on the system and to reconfigure the control law. The fundamental theory of fault diagnosis and FTC schemes are extensively explored in several references (Noura, Theilliol, Ponsart, Chamseddine, 2009) and will not be further discussed in this paper. The detailed modeling approach of fault diagnosis and tolerant control system integrated into the ORCs will be discussed in the future.

2.4 Software Development

In this work Matlab/Simulink based ORC analysis/ simulation tool, (call 'ORCAT' for convenience), has been developed with graphic user interface. ORCAT offers two different platforms: 'ORCAT' (Figure 8) for static analysis and 'ORCAT-DYN' for dynamic analysis. The development objectives of the software is to help manage the complexity of the system analysis which includes key components and cycle design, dynamic and control system analysis.

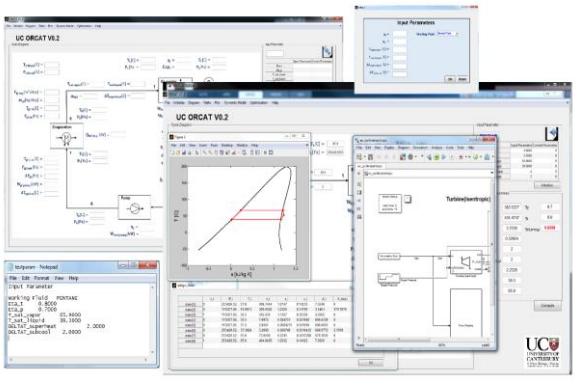

Figure 8 Steady State Analysis Tool

The ORCAT-DYN offers the Simulink libraries for system components such as heat exchanger, turbine, pump and etc. Each of the component blocks has the same interface delivering the fluid properties and other information so it can be replaceable in the system model. Thermodynamic properties are computed using REFPROP integrated into the custom Simulink library. The developing ORCAT-DYN library is shown in the Figure 9.

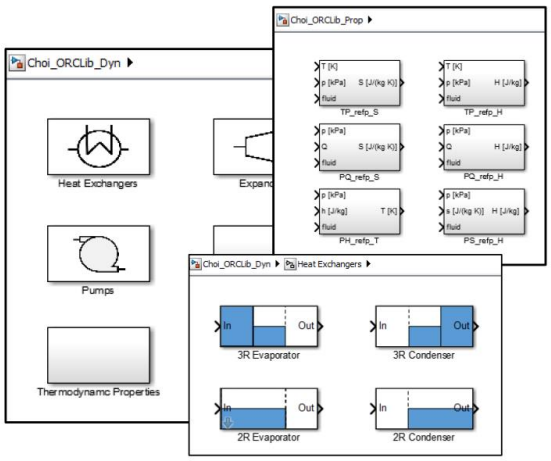

Figure 9 Modeling Library in Dynamic Simulation Tool

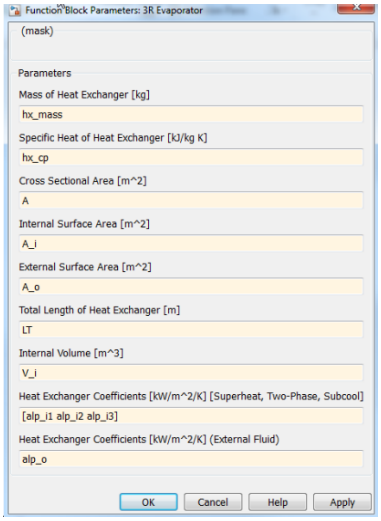

Figure 10 Masked Subsystem of Component

The main library is composed of 5 subcategory blocks: heat exchanger, expander, pump, miscellaneous tools, and thermodynamic properties. Each block contains subsystems associated with the subcategory. Any physical parameters and necessary information can be specified using a masked subsystem as shown in Figure.10.

2.5 System Model

Figure 11 shows ORC system model implemented using the developed model libraries. The connecting lines represent a flow signal which has information of flow properties such as pressure, enthalpy, mass flow rate and vapor fraction. To build a proper system model, each component has to be connected in a structured and logical manner through considering fundamental features of the cycle

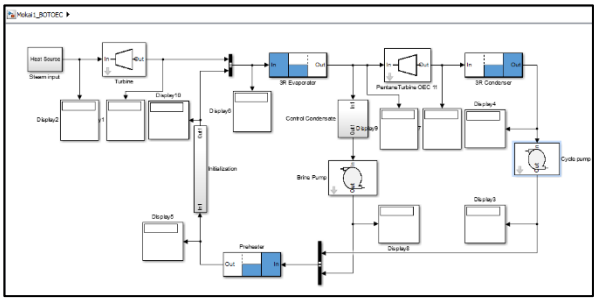

Figure 11 Modeling of ORC system using ORCAT-DYN

3. SIMULATION

In this section, we demonstrate the simulation of a heat exchanger model through a simple example. The example is representative of evaporator model with moving boundary approach. The physical parameters are adopted from the reference (Jensen, Tummescheit, 2002) for the simulation. The working fluid followed by the liquid pump is assumed entering the evaporator in liquid condition. The outlet is assumed to be vapor condition. The change of the length of subcooled (L_1), two-phase (L_2) and superheat (L_3) region are demonstrated in Figure 12. Figure 13 shows outlet enthalpy changes during the simulation

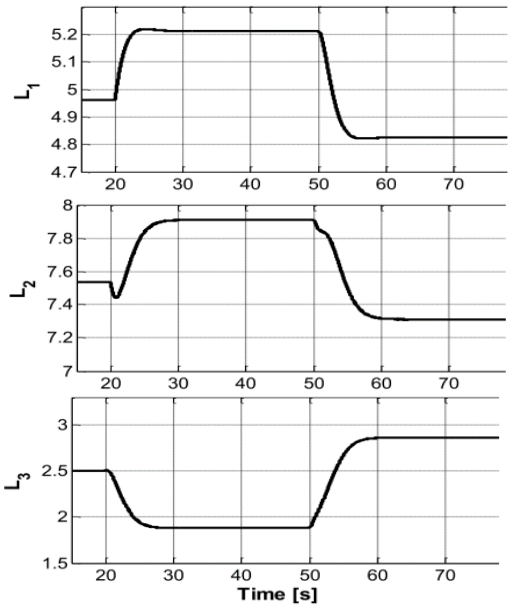

Figure 12 Lengths of Subcool (L_1), Two-phase (L_2), Superheat (L_3) Regions

The pump speed is increased by 5 % at time = 20 [s], which leads to increase in mass flow rate of the working fluid. The length of the subcooled and two-phase region is then starting to stretch and the outlet temperature of working fluid is dropped. The outlet heat transfer coefficient is increased by 10 % at time = 50 [s]. The amount of heat transferred through the wall is then increased which result in a decrease in the length of subcooled and two-phase region and rise in outlet enthalpy.

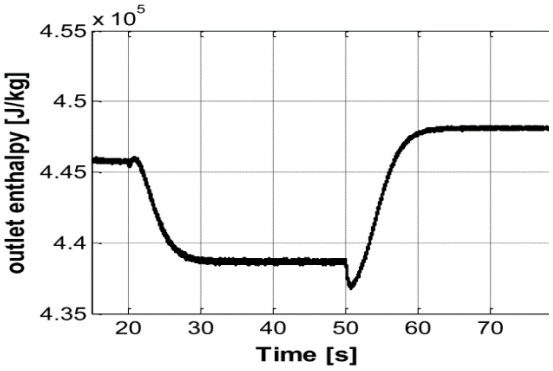

Figure 12 Outlet Enthalpy

4. CONCLUSIONS

A modeling strategy of dynamic system of ORC has been presented. The moving boundary approach for the heat exchanger has been explained with the case of condenser. A numerical test has been performed using the developed evaporator model which is derived from the same approach. A modeling and simulation tools have been developed to support system configuration, operation, diagnosis and design of the control system. Two different numerical frameworks based on steady state and dynamic regime is implemented under Matlab/Simulink environment along with graphic user interface.

APPENDIX

$$Q_{11} = A\rho_1(h_1 - h_g)$$

$$Q_{13} = AL_1\left[\left(\frac{\partial\rho_1}{\partial p}\Big|_{h_1} + \frac{1}{2}\frac{\partial\rho_1}{\partial h_1}\Big|_p \frac{dh_g}{dp}\right)(h_1 - h_g) + \frac{1}{2}\left(\frac{dh_g}{dp}\right)\rho_1 - 1\right]$$

$$Q_{21} = A(\rho_1 h_g - \rho_3 h_f)$$

$$Q_{22} = A\left[(\rho_g h_g - \rho_f h_f)\,\bar{\gamma} + (\rho_f h_f - \rho_3 h_f)\right]$$

$$Q_{23} = A\left[\left(\frac{\partial\rho_1}{\partial p}\Big|_{h_1} + \frac{1}{2}\frac{\partial\rho_1}{\partial h_1}\Big|_p \frac{dh_g}{dp}\right)h_g L_1 + \left(\frac{d(\rho_f h_f)}{dp}(1-\bar{\gamma}) + \frac{d(\rho_g h_g)}{dp}\,\bar{\gamma} - 1\right)L_2 + \left(\frac{\partial\rho_3}{\partial p}\Big|_{h_3} + \frac{1}{2}\frac{\partial\rho_3}{\partial h_3}\Big|_p \frac{dh_f}{dp}\right)h_f L_3\right]$$

$$Q_{24} = \frac{1}{2}AL_3 h_f\left(\frac{\partial\rho_3}{\partial h_3}\Big|_p\right)$$

$$Q_{31} = A\rho_3(h_f - h_3)$$

$$Q_{32} = A\rho_3(h_f - h_3)$$

$$Q_{33} = AL_3\left[\left(\frac{\partial\rho_3}{\partial p}\Big|_{h_3} + \frac{1}{2}\frac{\partial\rho_3}{\partial h_3}\Big|_p \frac{dh_f}{dp}\right)(h_3 - h_f) + \frac{1}{2}\left(\frac{dh_f}{dp}\right)\rho_3 - 1\right]$$

$$Q_{34} = \frac{1}{2}AL_3\left[\left(\frac{\partial\rho_3}{\partial h_3}\Big|_p\right)(h_3 - h_f) + \rho_3\right]$$

$$Q_{41} = A(\rho_1 - \rho_3)$$

$$Q_{42} = A\left[(\rho_g - \rho_f)\,\bar{\gamma} + (\rho_f - \rho_3)\right]$$

$$Q_{43} = A\left[\left(\frac{\partial\rho_1}{\partial p}\Big|_{h_1} + \frac{1}{2}\frac{\partial\rho_1}{\partial h_1}\Big|_p \frac{dh_g}{dp}\right)L_1 + \left(\frac{d\rho_f}{dp}(1-\bar{\gamma}) + \frac{d\rho_g}{dp}\,\bar{\gamma}\right)L_2 + \left(\frac{\partial\rho_3}{\partial p}\Big|_{h_3} + \frac{1}{2}\frac{\partial\rho_3}{\partial h_3}\Big|_p \frac{dh_f}{dp}\right)L_3\right]$$

$$Q_{44} = \frac{1}{2}AL_3\left(\frac{\partial\rho_3}{\partial h_3}\Big|_p\right)$$

$$Q_{51} = (C_p\rho V)_w\left(\frac{T_{w1} - T_{w2}}{L_1}\right)$$

$$Q_{55} = (C_p\rho V)_w$$

$$Q_{66} = (C_p\rho V)_w$$

$$Q_{71} = (C_p\rho V)_w\left(\frac{T_{w2} - T_{w3}}{L_3}\right)$$

$$Q_{72} = (C_p\rho V)_w\left(\frac{T_{w2} - T_{w3}}{L_3}\right)$$

$$Q_{77} = (C_p\rho V)_w$$

ACKNOWLEDGEMENTS

Supported by Department of Mechanical Engineering, University of Canterbury.

REFERENCES

Quoilin, S., Aumann. R., Grill, A., Schuster, A., Lemort, V. and Spliethoff, H.: Dynamic modeling and optimal control strategy of waste heat recovery organic rankine cycles. *Applied Energy, vol. 88, no. 6*, pp. 2183-2190. (2011).

Zhang, J., Zhang, W., Hou, G and Fang F.: Dynamic modeling and multivariable control of organic rankine cycles in waste heat utilizing processes. *Computer & Mathematics with Application, vol. 64, no. 5*, pp. 908-921. (2012).

Casella, F., Mathijssen, T., Colonna, P. and Buijtenen, J.: Dynamic modeling of organic rankine cycle power systems. *Journal of Engineering for Gas Turbines and Power, vol. 135, no. 4*, p. 042310. (2013)

Proctor, M.J., Yu, W. and Young, B.R.: Simulation of set-point feed-forward control of wellhead valves in an organic rankine cycle geothermal power plant. *Asia-Pacific Journal of Chemical Engineering, vol. 10, no. 4*, pp-501-511. (2015)

McKinley, T.L. and Alleyne, A.G.: An advanced nonlinear switched heat exchanger model for vapor compression cycles using the moving boundary method. *International Journal of Refrigeration, vol. 31, no. 7*, pp. 1253-1264. (2008).

Eldredge, B.D., Rasmussen, B.P. and Alleyne, A.G.: Moving boundary heat exchanger with variable outlet phase. *Journal of dynamic systems, measurement, and control, vol. 130, no. 6*, p. 061003. (2008)

Li, B. and Alleyne, A.G.: A dynamic model of a vapor compression cycle with shut-down and start-up operations. *International Journal of Refrigeration, vol. 33, no. 3*, pp. 538-552. (2010)

Jensen, J.M and Tummescheit, H.: Moving boundary models for dynamic simulations of two-phase flows. *Modelica 2002 Proceedings*, pp. 235-244. (2002).

MacArthur, J.W. and Grald, E.W.: Unsteady compressible two-phase flow model for predicting cyclic heat pump performance and a comparison with experimental data. *International Journal of Refrigeration, vol. 12, no. 1*, pp. 29-41. (1989)

Grald, E.W. and MacArthur, J.W.: A moving boundary formulation for modeling time dependent two phase flows. *International Journal of Heat and Fluid Flow, vol. 13, no. 3*, pp. 266-272. (1992).

Zhang, Z. and Yue, H.: Fault diagnosis and fault-tolerant control in power plants and power systems. *Measurement and Control, vol. 39, no. 6*, pp 171-177. (2006)

Noura, H., Theilliol, J., Ponsart., C. and Chamseddine, A.: Fault tolerant control systems: Design and practical applications. *Springer Science & Business Medea*. (2009)